



Green synthesis of silver nanoparticles from saline tolerant microalgae and their antiviral properties against HIV-1

Yuvaraj Sampathkumar ^{1*}, Elumalai Sanniyasi ¹, Mohana Priya Arumugam ², Pavithra Dhamodharan ², Selvaraj Palanisamy ³, Vikram Godishala ⁴, Madhusudhanan Jeyaraman ⁵, Vijayabaskar Pandian ⁶ and Kaushik Thamilchelvam ⁷

¹ Department of Biotechnology, University of Madras, Guindy Campus, Chennai - 600 025, Tamilnadu, India.

² Department of School of Bio Sciences and Technology, VIT, Vellore – 632014, Tamilnadu, India.

³ Department of Biochemistry & Biotechnology, Annamalai University, Annamalai Nagar -608002, Tamilnadu, India.

⁴ Department of Biotechnology, Ganapathi Degree College, Parakal-506164, Telangana, India.

⁵ Department of Biotechnology, Anand Institute of Higher Technology, Kazhipattur, Chennai-603003, Tamilnadu, India.

⁶ Government Theni Medical College & Hospital, Theni – 625 512, Tamilnadu, India.

⁷ Department of Research and Development, Quantee Data Tech Pvt. Ltd., Chennai - 600 086, Tamilnadu, India.

World Journal of Advanced Pharmaceutical and Life Sciences, 2022, 03(02), 024–034

Publication history: Received on 26 August 2022; revised on 25 October 2022; accepted on 27 October 2022

Article DOI: <https://doi.org/10.53346/wjapls.2022.3.2.0037>

Abstract

The microalgae were exposed to silver nitrate (AgNO₃) solution and screened for their suitability for production of the nano-silver (nano-Ag). The HIV-1 gag p24 Elisa Assay was used to study the anti-HIV activity of biogenic silver nanoparticles from microalgae *Nostoc sp.*, *Lyngbya sp.*, and *Phormidium sp.* The antiviral activity of biogenic silver compounds can be explained by their ability to cross the lipophilic membranes and interact with proteins involved in apoptosis. The antiviral activity of silver ion assembled into the V3loop of HIV -GP120. CD4 cell with CXCR4 chemokine receptor binding with its ligand CXCL12 plays an important role in protecting the entry of HIV virus. The role of the extracellular loop from CXCR4 and its mechanism allowed for the binding of HIV glycoprotein. This active site of protein bind with target protein to form protein–protein–ligand interaction to carry out the signals to lead the various pathways such as CXCL12 or SDF-1 protein-mediated kinase, Ras-c-Raf-1-MEK1/2-ERK1/2 dependent pathway, and CD45 cell-mediated pathway. The sulfur-bearing residues located in the glycoprotein knobs would be attractive sites for nanoparticle interaction. Silver nanoparticles are blocked the protease activity of different HIV-1 strains with overlooks their tropism. Modification in gp120 among HIV strains is the major determinant site of differing tropism among HIV strains.

Keywords: Biogenic silver nanoparticles; HIV-1; ELISA; Microalgae; CXCR4

1. Introduction

AIDS is a final stage of HIV infection that occurs when the body's immune system is suppressed by the action of HIV viruses. Statistical reports for the accounting of HIV infection were estimated 6,50,000 [5,10,000–8,60,000] people dying from HIV globally in 2021. The map showed the number of HIV-infected cases reported in 2017-18 with the top ten districts of Tamil Nadu [Fig. 1]. In most countries, HIV-infected persons are treated with anti-retroviral drugs [1] such as abacavir, emtricitabine, lamivudine, stavudine, tenofovir, and zidovudine but most of the HIV-1 strains are resistant to at least one of the available drugs. For these reasons, in need to the discovery of new anti-HIV agents that

* Corresponding author: Yuvaraj Sampathkumar

Department of Biotechnology, University of Madras, Guindy Campus, Chennai - 600 025, Tamilnadu, India.

function overcomes the retro transcription or protease activity that can be used for treatment and prevention of HIV/AIDS.

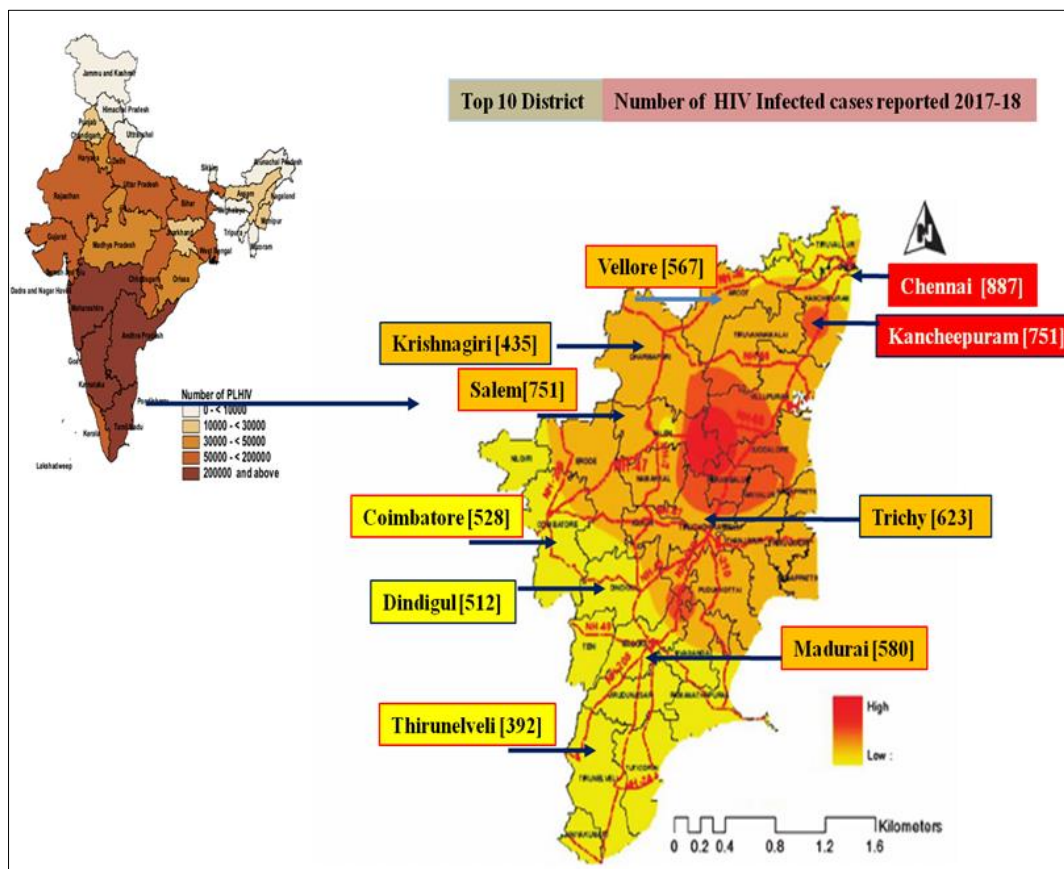


Figure 1 HIV infected reported on 2017-18 with top ten districts of Tamil Nadu

The virucidal [2] compounds differ from virstatin drugs in that they act directly and rapidly by lysing viral membranes on contact or binding to virus coat proteins. An example of Virucidal compounds is Sterillium, Dismozon R plus. The mechanism of HIV-inhibitory activity of silver nanoparticles was not clearly studied. Silver particles have antimicrobial properties, but their medical applications declined with the development of antibiotics. Nowadays, silver sulfadiazine [3] [4] [23] compound is listed by the World Health Organization as a crucial anti-infective topical medicine. Silver's mode of action depends on the Ag⁺ ions, which strongly inhibit bacterial growth through the elimination of respiratory enzymes and electron transport components and through interference with DNA functions.

1.1. Human chemokine CXCR4

The chemokine receptor CXCR4 [5] [6] is a type of G-protein-coupled molecule expressed on the surface of an enormous number of cells such as T-lymphocytes, monocytes, neutrophils, dendritic, endothelial cells, primordial germ cells, skeletal muscle satellite progenitor cells, neural stem cells, stem cells, retinal pigment epithelium progenitor and murine embryonic stem cells.

1.2. Chromosomal map and gene Map

The cytogenetic location of CXCR4 [Fig. 2] 2q22.1, which is the long (q) arm of chromosome 2 at position 22.1. The CXCR4 gene structures were characterized, find the promoter region, and determined the genomic structure of the human gene [Fig. 3]. The CXCR4 [7] gene contains two exons' regions have separated by an intronic sequence. A 2.6 kb 5P-flanking sequence located at upstream of CXCR4 [5]. The open reading frame contains a TATA box or Pribnow box (also known as the Pribnow-Schaller box) is a sequence of TATAAT of six nucleotides precedes the transcription-initiation site and regulation of transcription start at 5' UTR region to 3' UTR region by binding of RNA transcriptase enzyme used to study the characteristic function of a promoter. This region also contains putative consensus binding sequences for the binding of different transcription factors, some of them associated with the production of blood cells and platelets which occurs in the bone marrow and lymphocyte development.

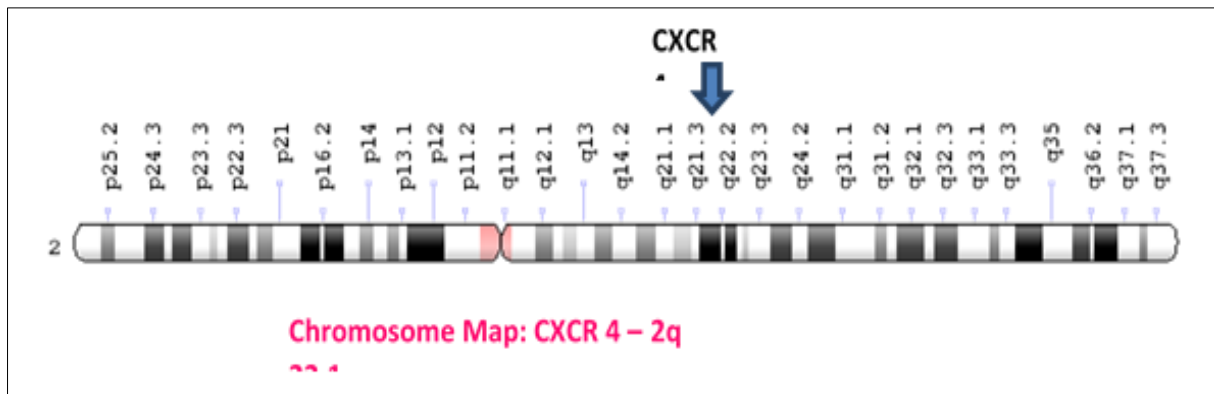


Figure 2 Chromosomal and gene map of CXCR4

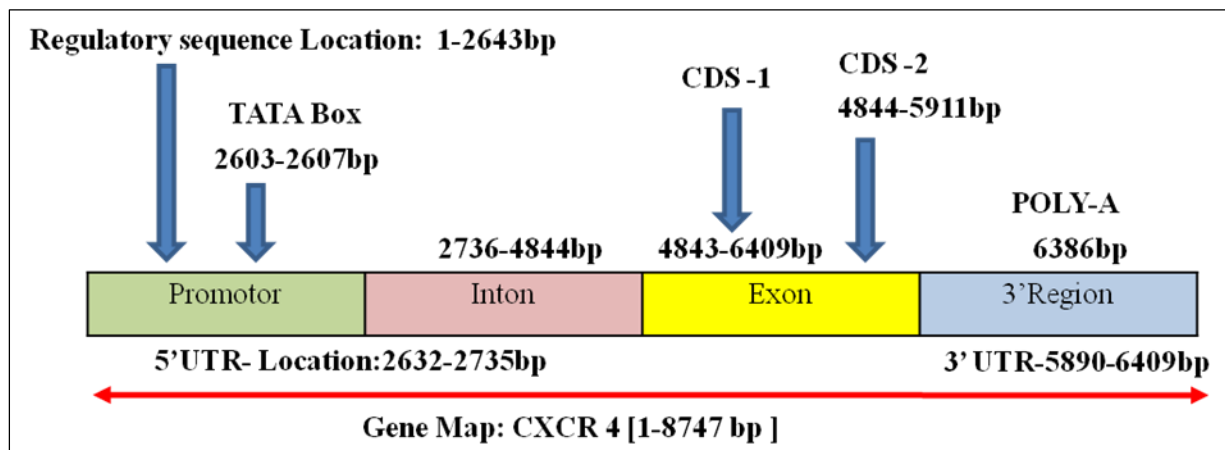


Figure 3 Gene map of CXCR4

1.3. CXCR4

C-X-C chemokine receptor type 4 otherwise called CD184 antigen or chemokine (C-X-C motif) receptor 4 or CXCR4_HUMAN or D2S201E or FB22 or Fusin or HM89 or HSY3RR or LAP-3or LAP3or LCR1or LESTR or leukocyte-derived or seven-transmembrane domain receptor or lipopolysaccharide-associated protein 3 or LPS-associated protein 3 or neuropeptide Y receptor Y3 or NPY3R or NPYR or NPYRL or NPYY3R or SDF-1 receptor or seven transmembrane helix receptor or seven- transmembrane-segment receptor and spleen stromal cell-derived factor 1 receptor. The seven transmembrane helix receptor surfaces suggest that has a greater implication of the N-terminus and the three extracellular loops are ECL1, ECL2 [8] [9], and ECL3 located in the ligand binding and receptor activation. The 3D-dimensional structure of chemokines receptor which is consists of an elongated and flexible N-terminus, cysteine-rich repeats domain, a loop of approximately ten residues, often referred to as the N-loop, a single-turn of 3.10 helix with three anti-parallel β -strands and a C-terminal α -helix. The secondary structures of CXCR4 are connected by helix turns known as the 30s, 40s, and 50s ECL loops, which analyze the numbering of residues in the mature protein. The chemokine CXCR4 protein structure is further balanced by assemblies of two disulfide bridges on the cysteine residues at the N-terminal end with those located on the 30s and 50s loops. In our study, we investigated that neutralizing the properties of individual peptides were corresponding to the extracellular loops ECL1, ECL2, and ECL3.

Chemokines carry the cysteines repeat domain and fall into four families defined by a cysteine signature motif: CXC, CC, C, or CX3C where C is a cysteine and X any amino acid residue. CXCR4 receptor proteins have specific sites into which certain other proteins, called ligands, fit like keys into locks. After attachment of its ligand, called CXCL12 or SDF-1, the CXCR4 protein turns on to activate the signaling pathways inside the cell. The chemokine CXCR4 receptor is binding with its unique endogenous CXCL12. This interaction plays an important role in various mechanisms such as T cell activation and proliferation, hematopoietic stem cell, development of leukocyte trafficking, and production of cytokine and other proteins. Expressions of CCR1, CCR2or CCR5 chemokines were induced by IL2, but are down-regulated by lectin or T cell-specific activators. Expression of IL8 receptors in lymphocytes by IL2 or activation of CD3 mediated cell signaling. CXCR4 is the only receptor capable of binding to SDF1 and permitting cell signaling to prevent HIV entry in

host cells and promoting endocytosis. CXCL12 or SDF-1 stimuli activate receptor interaction with CXCR4 protein for the production of trimeric G-Protein. The trimeric G-protein contains alpha, beta, and gamma units. These proteins were carried out the phosphorylation process to convert the GDP to GTP for assembly of G protein alpha subunits and the dissociation of the beta or gamma protein. G alpha-protein directly stimulates the kinase activity by a down-regulated mechanism. Src families of tyrosine kinase protein is bound to the catalytic domains to change the conformation. These conformational changes activate the Ras-c-Raf-1-MEK1/2-ERK1/2 [10] dependent pathway through phosphorylation of adaptor protein Shc, adaptor protein GRB2 and SOS protein are leading to raise the transactivation potential of Elk1 transcription factor and the repressed state transactivation ability of transcription factor STAT3 which both are phosphorylated by ERK2 SDF-1alpha activates the JAK/STAT pathway. JAK2 is activated and associated with the CXCR4. CD45 receptor-mediated dephosphorylation mechanisms in the Src family kinases to activate Fyn and Lck protein. The activated Lck proteins promote the guanine nucleotide exchange factor VAV1. VAV1 protein activates the RhoA, Rac1, and CDC42 that are involved in actin cytoskeleton reorganization. SDF-1-CXCR4 signaling plays an important and unique role in the regulation of stem or progenitor cell trafficking, inflammation, embryogenesis, organogenesis, and tissue regeneration. The combination of SDF-1 protein with CXCR4 chemokines were stimulating the various signaling pathway. HIV envelopes proteins are overcome the immune mechanism of the host cell via CXCR4 or CCR5. The mutation on the CXCR4 receptor will permit the entry of HIV entry into the host.

1.4. *In silico* study of nanoparticles

Silver nanoparticles are used in various biological applications such as molecular diagnostics, photonic devices, nano-medicine drug delivery, imaging diagnostics, and biosensing. Quantum mechanics calculations are one of the best methods for investigating silver nanoparticles. Computational modeling is a powerful tool compared with experimental analysis because of its limitations in working conditions. The computational works are possible to manage every parameter separately to identify the all mechanism i.e., responsible for the experimental result. With a computational analysis, it is possible to simulate interactions under different conditions that are not always possible to be studied in the lab. The nano-materials are size-dependent because their physical and chemical properties will depend on the size of the nanoparticle. The composition, size, shape, texture, and environment of nanoparticles can strongly influence their ultimate application in various fields such as antimicrobial coatings, textiles, keyboards, wound dressings, and biomedical devices. Ab initio calculations and density functional theory (DFT) method which is used to study the affinity of silver ions with DNA at a molecular level were performed to determine the interaction of silver ions with cytosine and adenosine base structures. And another important study is the interaction between nanoparticles and the lipid layer. *In silico* computational study was performed to determine the compounds to visualize the structural information. The research work is focused on the 3D and quaternary structure of GP 120 molecules with silver nanoclusters. In previous works, small silver clusters were studied using DFT [11] methods for the ground state geometries and binding energies per atom of small silver clusters, from 4 to 8 silver atoms by Poteau and his team workers. With their results to manage the parameterize distance-dependent [12] tight-binding Hamiltonian kinetic energy polished with good correlation between their model and ab initio calculations. Today, nano-materials or multi-metallic clusters ions [13] and their compounds are creating an interest in a wide range of properties by adding two or more chemical elements, which often enhanced better catalytic reaction than the pure metals. In a theoretical study, the results by density functional theory showed that the doping of Au atoms improved the stability of Ag–Au clusters. The Gupta potential, as formulated by Cleri & Rosato, is adopted to describe the interatomic interactions in bimetallic Ag–Au. A combination of global optimization, i.e., Birmingham cluster genetic algorithm (BCGA), and DFT [14] calculations were applied to study Ag–Au clusters. Odd number and even number methods are used to study the tight-binding Hamiltonian kinetics. Results showed that the transition state from two to three (2D or 3D) dimensional structures is predicted between Au₆Ag₂ [3:1] even number method and Au₅Ag₃ [5:3] odd number method, and the atomic ordering in core/shell structures was found to be related to the electric dipole moment. There existed an apparent tendency for surface segregation of the Ag atoms in 38-atom Ag–Au clusters [even number method], and the stability of clusters was related to the increasing number of Au–Au and Ag–Au bonds. In the stable structures of [14] Ag–Au clusters containing 20–150 atoms (with atomic ratio 1:1), decahedra (Dh) and icosahedra (Ih) were the main motifs, and Ag₄₄-Au₄₄ cluster was deemed to have high structural, electronic and thermal stability. Furthermore, a clusters expansion model was used to determine the chemical ordering of 114-atom and 309 –atoms Ag–Au Mackay icosahedral nanoparticles. Structures of nano-Au and nano-Ag clusters can be categorized into dihedral, icosahedra, face cubic centered, and Teary tetrahedral, and the strong nanocluster bond.

1.5. Silver ion and silver cluster –GP protein interaction:

The antiviral properties of silver nanoparticles against HIV-1 by invitro biotin-streptavidin labeled enzyme assay, the images were obtained by high angle annular dark field [HAADF] and scanning transmission electron microscopy [STEM] showed that gp120 as its possible molecular target. An advanced microscopy technique is used to study the regular spatial arrangement of the silver nanoparticles attached to HIV-1virions. The center-to-center distance between the

silver nanoparticles [~ 28 nm] was similar to the spacing of gp120 spikes over the viral membrane [~ 22 nm]. It was considered that the defined sulfur-bearing residues [25] [Fig. 4] [Methionine, cysteine, homocysteine, and taurine are the 4 common sulfur-containing amino acids, but only the first 2 are incorporated into proteins] located in the glycoprotein knobs would be attractive sites for nanoparticle interaction. Silver nanoparticles have controlled the activity of different HIV-1 strains with overlooking their tropism. Modification in gp120 among HIV strains is the major determinant site of differing tropism among HIV strains. The V3 loop of gp120 protein encounters the chemokine receptors CXCR4 [T-tropic virus], CCR5 [M-tropic virus], or both [dual-tropic virus]. The appearances of silver nanoparticles inhibit the mode of action in HIV 1 activity.

2. Material and methods

2.1. Sample Collection

Silver nitrate (AgNO_3) Chemicals were purchased from Sigma-Aldrich (India), the isolated Cyanobacterial species were cultured in BG11 medium under 3000 lux light intensity with the static condition, for 12 h under illumination and 12 h under darkness, culture was shaken manually twice in a day. Microalgal cultures were harvested approximately after a production period of 21 days and used for the synthesis of biogenic silver nanoparticles. Further studies based on the morphological appearance and Taxonomic classification of the microalgal isolates were identified.

2.2. Synthesis of Silver Nanoparticles (Ag-NPs)

The culture of microalgal strain growing in BG11 medium was harvested by centrifugation and these pellets were washed with sterile water and sonicated in an EQUITRON ultrasonic cleaner for 15 min at maximum output and duty cycle. The extract was critically examined microscopically to ensure complete breakage of the cells; if the extract showed the presence of filaments/cells, steps of sonication were repeated. If needed, the extract was incubated at 2-4°C overnight to attain complete lysis of cells. The resulting cell-free extract was centrifuged at $10,000 \times g$ for 15 min and filtered through Whatman No. 1 filter paper to eliminate cell debris if any for the synthesis of [17][19][20] [21] [22] AgNPs, the cell extract was distributed equally (50 ml each) into two flasks. In one flask, silver nitrate (AgNO_3) was added to obtain a final concentration of 1 mM, the other flask contained only cell extract and served as the positive control. Pure AgNO_3 solution (1 mM) was taken in a flask separately for negative control. All the flasks were wrapped in aluminum foil to make sure complete darkness and incubated at 25°C in a shaker (200 rpm) for 72 hrs. During the incubation period change of the brown color indicates silver nanoparticle synthesis.

2.3. Atomic Force Microscopy (AFM)

A thin film of the sample was prepared on a glass slide (1mm square) by dropping 300 μl of the sample on the slide, allowed to dry for 30 minutes and the slides were then scanned with AFM [15][16] [18] (NT-MDT, NTEGRA PRIMA – Ireland). The AFM characterizations were carried out in ambient temperature in non-contact mode using silicon nitride tips, varying resonance frequencies with integrated optical viewing system and just find out the correct locations to measure and magnified in to target your SPM tip on that particular area than control the scanning process in real-time and compare an optical image with Image processing software for AFM [Mountain-®- premium and expert tool -Digital Surf, France] was used to obtain the 2D and 3D image acquisition, from data management to scientific art creation.

2.4. Anti-HIV activity

Anti-HIV testing of the extract was done by a cell-free method as described before [24] (Wang et al., 2008). Briefly, 1 mg/ml concentrations of the biogenic synthesized silver nanoparticles or control agents were pretreated with 15 μg of virus and incubated for 1 hour at 37°C. After this, the virus/ biogenic silver nanoparticles mixture was added to MT-2 or PBMC cells (0.3×10^6 cells) and incubated at 37°C for 2 hours. Cells were washed and re-suspended in 2 % RPMI and further incubated for 5 days at 37°C. Cells were divided into 3 groups namely drug-positive control treated with Nonoxynol-9, group treated with distilled water (drug-negative control), and test group. After 5 days, the supernatants were collected and tested for HIV gag p24 content by ELISA (Xpress Bio Cat. No.1000). The blasted PBMC different concentrations of algal samples were added (100 μl) in serial dilution (from 5mg/ml to 1 μg /ml) and incubated for 5 days.

2.5. Molecular visualization of HIV protein

In the present work, we describe a plug in Pymol which allows to carry out virtual screening with Pymol. The visualization is crucial for structure-based drug design. Pymol is the most frequently used programme for generating publication quality picture of molecular structure. It is easy to handle autodock/vina-plugin for Pymol is expected to who are not docking expert to make use of these docking protocol with their preferred environment. The size and

location of this binding site is visualized in Pymol and can be adjusted interactively. Down load the software installation file from Unofficial Windows Binaries for Python Extension Packages. Download "pymol-1.6.0.0.win32-py2.7.exe" updates. Unzip the file then double click on the Run "pymol-1.6.0.0.win32-py2.7.exe" to begin the installation process. Choose Python Install directory (C:\Python27\PyMOL) software and follow the on-screen installation of the installation wizard. To open the PDB file, select "File Open" in the external GUI window, and select the 2BAC and 5CAY PDB file that you downloaded. The PDB file will load, and you will see the representation of the protein.

3. Results and discussion

The microalgae samples were observed under microscope, photographed and morphologically identified micro algal such as *Nostoc* sp. *Lyngbya* sp. and *Phormidium* sp. [Fig. 4, 5 and 6]. *Nostoc* is a filamentous form of both terrestrial and aquatic habitats. Trichome resembling a string of beads. Large colonies of closely packed trichomes enclosed by their mucilaginous sheath. Cells are rounded or oval cells. At frequent intervals along with the trichome terminal or in intercalary position heterocyst are found. *Lyngbya* is a unicellular, Filamentous; thick, rarely solitary, rarely tangled into free clusters of coiled filaments, firm sheaths, which are sometimes layered or stratified and brownish colored, opened at the ends; asexually reproduction (hormogonia); barrel-shaped discoid, cell content blue-green, olive green, yellowish, brownish or pinkish, with coiled thylakoids, situated more or less over the whole cell content; a thickened cap on the terminal cell of a cyanobacterial filament. Heterocyst and Akinetes are absent. *Phormidium* sp. usually forms flat, slimy mats of tangled filaments. The filaments are long, cylindrical, and may be curved or spiraled. Thin, firm, colorless sheaths adhere closely to out growths or appendages on *Phormidium* cells. The apical cells may have calyptra with more pointed, narrow or spherical than the other cells.

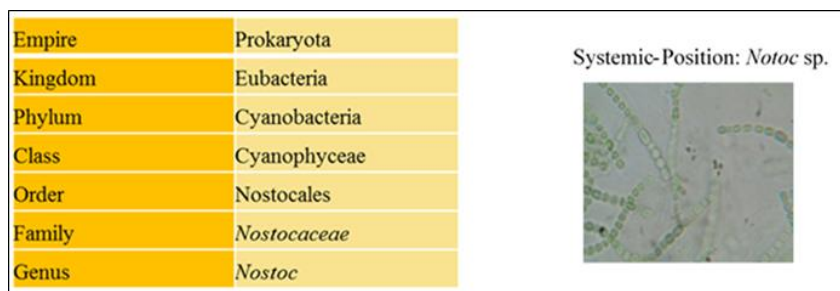


Figure 4 *Nostoc* sp

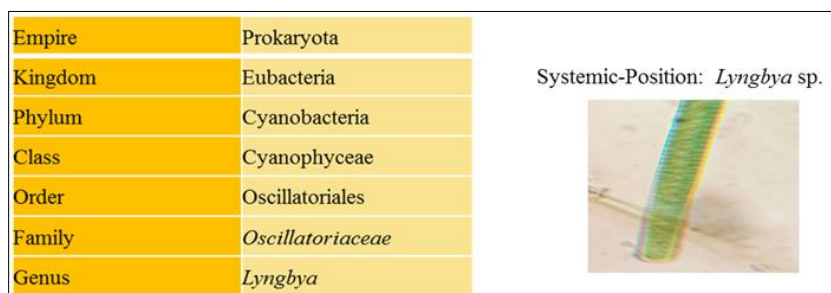


Figure 5 *Lyngbya* sp

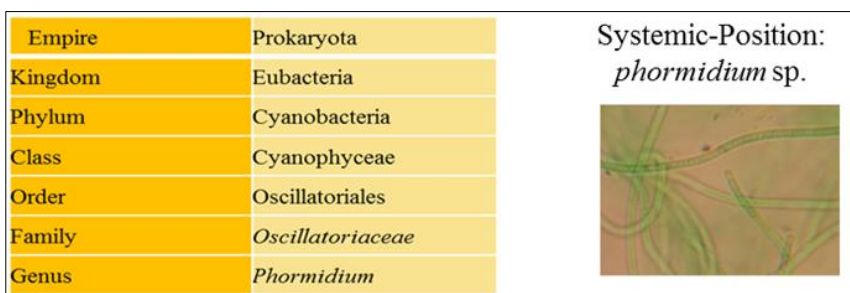


Figure 6 *Phormidium* sp

3.1. Analysis of silver nanoparticle in AFM

The obtained morphology revealed the fact that the synthesized silver nanoparticles are almost spherical silver nanoparticles obtained from AFM (NT-MDT, NTEGRA PRIMA –Ireland) has a broad size distribution in the range of nanometers, which also can be correlated with the observed broad area of the absorbance peak. The particles are mono disperse [Table 1] but seem agglomerated as this could be because the presence of some important bio-organic compounds in the microalgal extract seems to act as a ligand which effectively stabilizes the formed silver nanoparticles shown in Fig. 7 and 8. (AFM 3D-images of biogenic silver nanoparticle from *Nostoc* sp., *Lyngbya* sp and *Phormidium* sp. A: 10 nm, B: 15 nm, C: 4 nm).

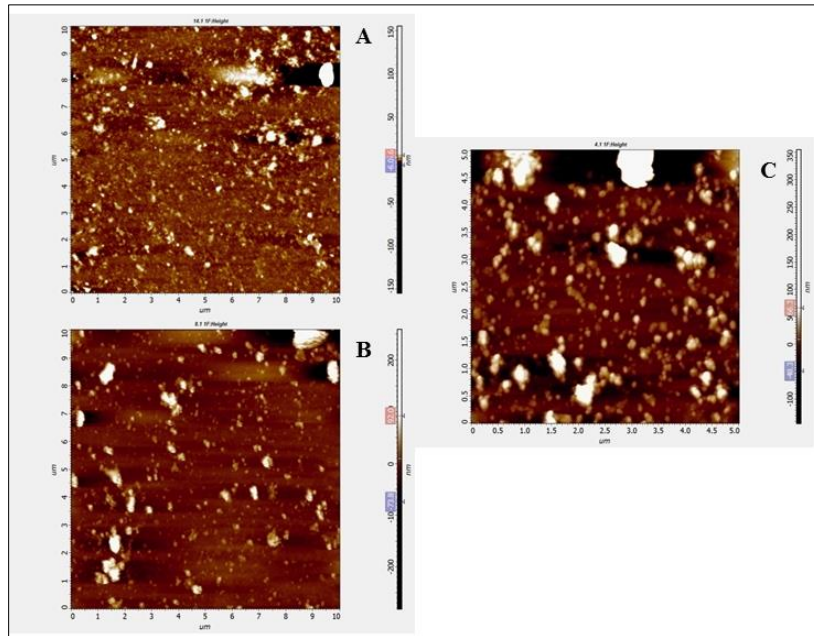


Figure 7 2D images of biogenic silver nanoparticle in microalgae (A: *Nostoc* sp., B: *Lyngbya* sp and C: *Phormidium* sp.)

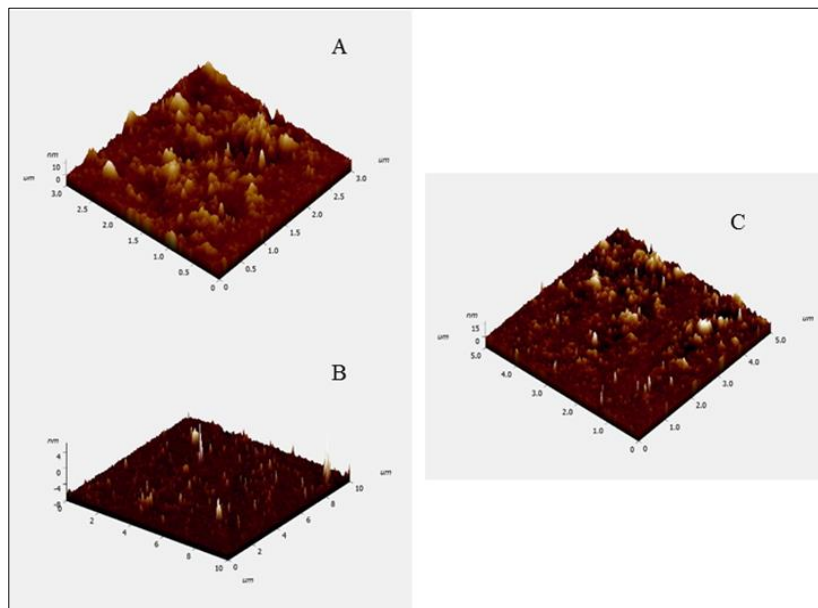


Figure 8 3D images of biogenic silver nanoparticle microalgae (A: *Nostoc* sp., B: *Lyngbya* sp and C: *Phormidium* sp.)

Table 1 Biogenic silver nanoparticle size height and depth

Silver compound: Biogenic silver nanoparticles	<i>Nostoc</i> sp. – AgNPs	<i>Lyngbya</i> sp.- AgNPs	<i>Phormidium</i> sp.- AgNPs
Size	30 nm	40 nm	80 nm
Height	6.7 nm	27.7 nm	36 nm
Depth	-9.3 nm	-20.8 nm	-26.6 nm

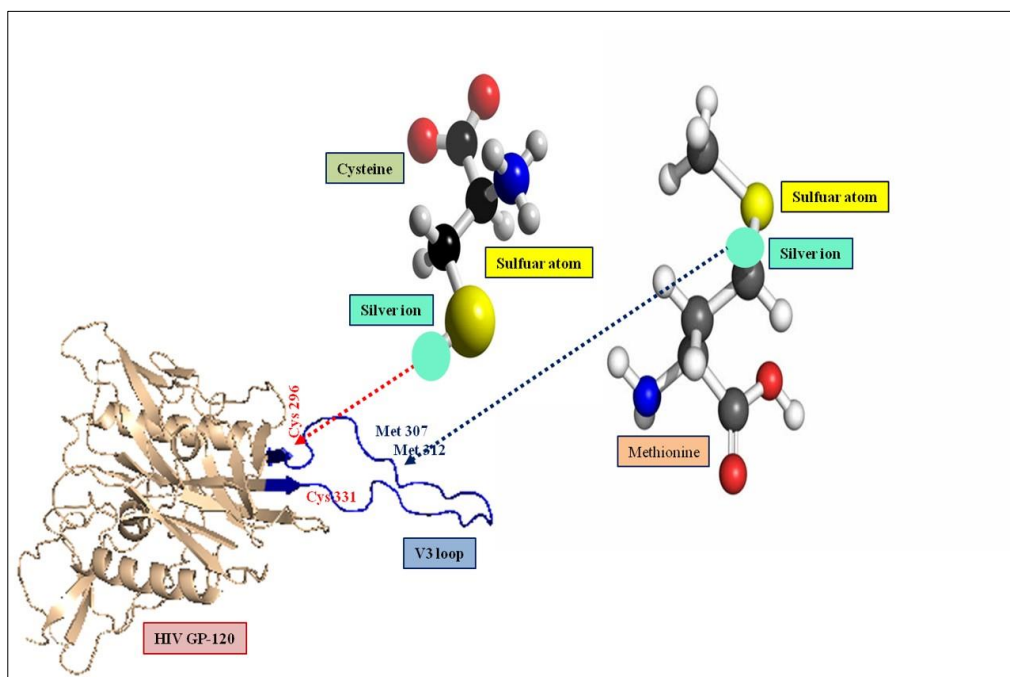
3.2. Anti-HIV activity: Inhibition of Gag p²⁴ –BT-2/PBMC interaction.

Biogenic silver nanoclusters were shown to be more stable than silver ions. The Cell viability in MT-2 cell or PMBC (IC₅₀) values were measured for the biogenic silver nanoparticles from *Nostoc* sp. *Lyngbya* sp. and *Phormidium* sp. Shown in Table 2.

Table 2 Inhibitory effect of biogenic silver nanoparticles against HIV-1

S.NO	Biogenic AgNPs	concentration	Cell viability in MT-2 cell or PMBC (IC ₅₀ *)
1.	<i>Nostoc</i> sp.	1.0	74.9
2.	<i>Lyngbya</i> sp.	1.0	62.3
3.	<i>Phormidium</i> sp.	1.0	67.4

3.3. *In silico* studies of GP120 vs silver ion binding complex

**Figure 9** HIV-1 GP120 (2B4C) is represented here as a cartoon model and V3 loop was represented in blue colour

The Pymol was the most frequently used programme for generating publication quality pictures of molecular structure. It was easy to handle autodock / vina-plugin for Pymol was expected to those who are not docking experts to make use of these docking protocol with their preferred environment. The size and location of this binding site was visualized in Pymol and can be adjusted interactively. Silver nanoparticles were controlled the activity of different HIV strains with overlooks their tropism. Modification in GP120 among HIV strains was the major determinant site of differing tropism among HIV strains. The structure of HIV envelope glycoprotein 120 was retrieved from the RCSB PDB database. The x-ray crystal structure of 2B4C was used in this representation Fig. 8. The third variable loop residues play a vital role in the formation of amino acid-Ag ion binding complex and complex values are discussed in Table 3 [26]. It was considered

that the defined sulfur-bearing residues [Methionine, cysteine, homocysteine, and taurine] are the 4 common sulfur-containing amino acids, but the first two sulfur-bearing residues were rapidly attracted to the silver ions and incorporated into V3 loop located in the glycoprotein knobs would be attractive sites for nanoparticle interaction. In 2B4C protein third variable loop region was grey colour, and their acidic and sulfur-bearing residues were highlighted and labelled in a different colour [Fig. 9 and 10]. The acidic and sulfur-bearing residues such as CYS296, ASN300, GLN301, ASN302, GLY312, GLY314, GLY321, GLU322, GLY324, ASP325, GLN328, and CYS331 from V3 loop, attract the silver nanoparticles to the interaction effects in HIV1. In 5CAY protein third variable loop region was grey colour and their acidic and sulfur-bearing residues were highlighted and labelled in a different colour [Fig. 11]. The acidic and sulfur-bearing residues such as ASN302, ASN306, CYS311, and GLY315 from V3 loop, attract the silver nanoparticles to the interaction effects in HIV2.

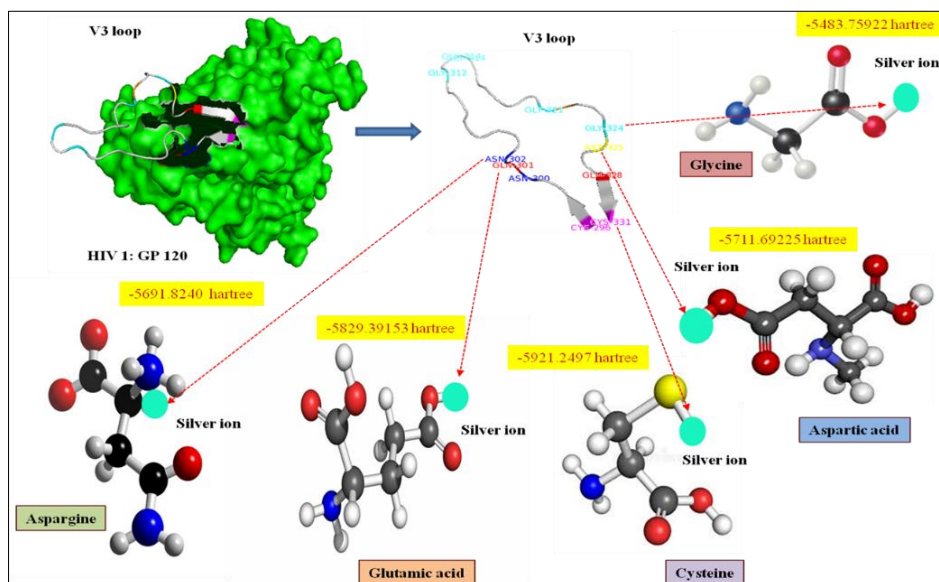


Figure 10 Human immune deficiency virus-1 (HIV-1) glycoprotein 120 (2B4C) is represented as surface model (green) and their third variable loop region (V3) is represented as cartoon model (grey) using Pymol. The acidic and sulfur bearing amino acid residues is highlighted

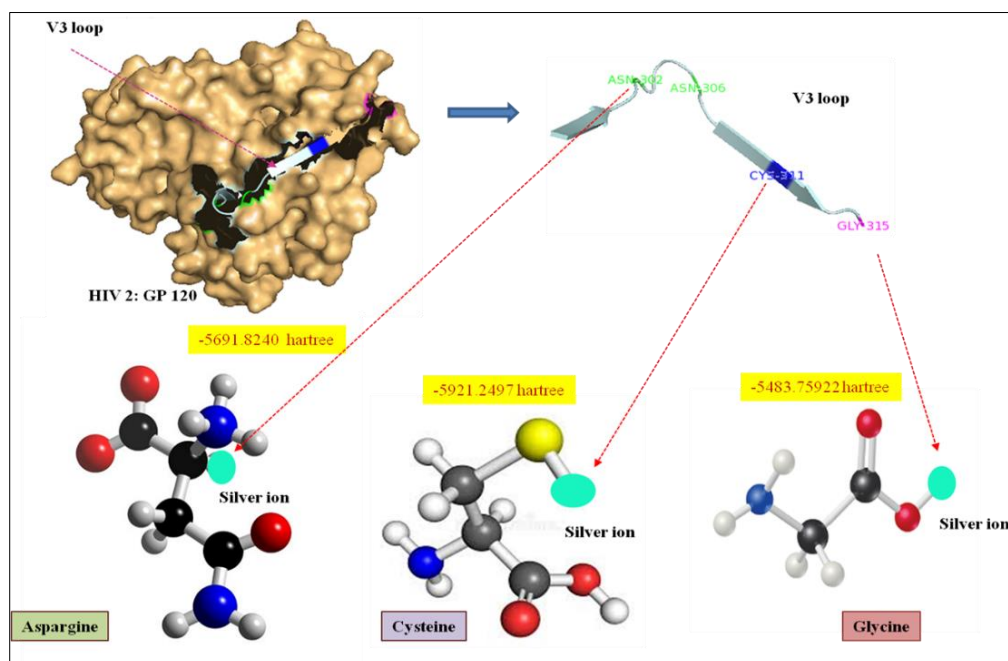


Figure 11 Human immune deficiency virus-2 (HIV-2) glycoprotein 120 (5CAY) is represented as surface model (orange) and their third variable loop region (V3) is represented as cartoon model (grey) using Pymol. The acidic and sulfur bearing amino acid residues is highlighted

Table 3 Energy binding value of Ag⁺ - amino acid complex of V3 loop [26]

Ag ⁺ -aminoacid complex	Energy (hartrees)	ZPE (Kcalmol ⁻¹)	H ^o 298-H ^o (Kcalmol ⁻¹)	Entropy (cal ^k - ¹ mol ⁻¹)
Ag ⁺ -Glycine	-5483.75922	51.8	5.0	86.5
Ag ⁺ -Cysteine	-5921.2497	69.3	6.7	99.9
Ag ⁺ -Aspartic acid	-5711.69225	78.9	7.4	106.5
Ag ⁺ -Glutamic acid	-5751.01135	97.1	8.2	112.0
Ag ⁺ -Asparagine	-5691.8240	86.5	7.7	108.1
Ag ⁺ -Methionine	-5999.89117	106.1	8.5	113.4

4. Conclusion

In conclusion, we report a green chemistry approach is an eco-friendly method for the synthesis of silver nanoparticles (Ag-NPs) using marine algae. These methods are quite stable in solution. The small nano-cluster or nano-silver ions were assembled on the sulfur-bearing residues region and of GP-120. The length of the gp120 V3 loop is relatively conserved at about 35 amino acids. Silver nanoparticles are a high affinity to cysteine and methionine amino acids because of the presence of their free SH binding site at Cys-296, Cys-331, Met-307, and Met 312. The Dihedral cluster motif is reliable and strong confirmation state than the other. The dihedral Ag-nanoclusters were assembled at the V3 loop and its antiviral mechanisms against HIV-1. Further, the synthesized biogenic nanoparticles would be used for biomedical application of cancer therapeutics, coating medicinal devices, anti-bacterial & anti-viral masks, anti-radiation fabric materials, silver ink, and dental material.

Compliance with ethical standards

Acknowledgments

The authors gratefully acknowledge the Dr. Mageshkumar, CLRI-center for analysis, testing evaluation and reporting services [CATERS].

Disclosure of conflict of interest

Conflict of interest declared none.

References

- [1] Margot N.A., Waters J.M., and Miller M.D. In Vitro Human Immunodeficiency Virus Type 1 Resistance Selections with Combinations of Tenofovir and Emtricitabine or abacavir and Lamivudine. *Antimicrobial agents and chemotherapy*. 2006 50: 4087–4095.
- [2] Humberto H Lara1, Elsa N Garza-Treviño, Liliana Ixtepan-Turrent, and Dinesh K Singh. Silver nanoparticles are broad-spectrum bactericidal and virucidal compounds. *Journal of Nanobiotechnology*. 2011. 9: 30.
- [3] Joy Fong Fiong wood. Nanocrystalline silver dressing in wound management. *International journal of nanomedicine*. 2006 1(4):441-449.
- [4] Stefania Galdiero, Annarita Falanga, Mariateresa Vitiello, Marco Cantisani, Veronica Marra and Massimiliano Galdiero. Silver Nanoparticles as Potential Antiviral Agents. *Molecules*. 2011 16: 8894-8918.
- [5] Stefania Scala, Crescenzo D'Alterio, Samantha Milanese, Alessandra Castagna, Roberta Carriero, Floriana Maria Farina, Massimo Locati, and Elena Monica Borroni. New Insights on the Emerging Genomic Landscape of CXCR4 in Cancer: A Lesson from WHIM. *Vaccines*. 2020 8(164):1-25.
- [6] Lauren E. Heusinkveld Shamik, Majumdar Ji, Liang Gao, David H. McDermott, Philip M. Murphy. WHIM Syndrome: from Pathogenesis Towards Personalized Medicine and Cure. *Journal of Clinical Immunology*. 2019 39:532–556.
- [7] Mouriuchi M, Mouriuchi H, Turner W, and Fauci A.S. Cloning and analysis of the promoter region of CXCR4, a coreceptor for HIV-1 entry. *The journal of immunology*. 1997 159(9):4322-4329.

- [8] Donald J. Chabot and Christopher C. Broder. (2000). Substitutions in a Homologous Region of Extracellular Loop 2 of CXCR4 and CCR5 Alter Coreceptor Activities for HIV-1 Membrane Fusion and Virus Entry. *JBC Papers in Press*. 2000 275:23774-23782.
- [9] Brian J. Willett, Karen Adema, Niolaus Heveker, Anne BreLOT, Laurent Picard, Marc Alizon, Julie D. Turner, James A. Hoxie, Stephen Peiper, James C. Neil, And Margaret J. Hosie. The Second Extracellular Loop of CXCR4 Determines Its Function as a Receptor for Feline Immunodeficiency Virus. *Journal of virology*. 1998 72(8):6475-6481.
- [10] Patrick R. O'Neill, W. K. Ajith Karunarathna, Vani Kalyanaramana, John R. Silvius, and N. Gautama. G-protein signaling leverages subunit-dependent membrane affinity to differentially control $\beta\gamma$ translocation to intracellular membranes. *PNAS plus*. 2012 E3568–E3577.
- [11] Andrea Fabara, Sebastián Cuesta, Fernanda Pilaquinga, and Lorena Meneses. Computational Modeling of the Interaction of Silver Nanoparticles with the Lipid Layer of the Skin. *Hindawi Journal of Nanotechnology*. 2018 (29):1-9.
- [12] Jijun Zhao. Tight-binding molecular dynamic study of silver clusters. *International Centre for Theoretical Physics*. 1999 14(3):309-316.
- [13] Rene Fournier. Theoretical study of the structure of silver clusters. *Journal of chemical physics*. 2000 115: 2165-2177.
- [14] Rongbin Du, Sai Tang, Xia Wu, Yiqing Xu, Run Chen, and Tao Liu. Theoretical study of the structures of bimetallic Ag–Au and Cu–Au clusters up to 108 atoms. *Royal society publishing*. 2019 6:190342.
- [15] S. K. Dora. Atomic Force Microscopy as a Quantitative Tool for Particle Characterization: From Microns to Angstrom Scale. *International Journal of Advanced Engineering and Nano Technology*. 2017 7:10-14.
- [16] Francesco Marinello. Atomic force microscopy in nanometerology: Modelling and enhancement of the instrument. *Padava Digital University Archive*. [Ph.D Thesis] 2006 1-175.
- [17] Mrinal Kashyap, Kanchan Samadhiya, Atreyee Ghosha, Vishal Ananda, Parasharam M. Shirage, and Kiran Bala. Screening of microalgae for biosynthesis and optimization of Ag/AgCl nano hybrids having antibacterial effect. *RSC advances*. 2019 9:25583-25591.
- [18] Kai-Chih Chang, Yu-Wei Chiang, Chin-Hao Yang, Je-Wen Liou. Atomic force microscopy in biology and biomedicine. *Tzu Chi Medical Journal*. 2012 162-169.
- [19] Prerna Khan, Amrit kaur, and Dinesh goyal. Algae based metallic nanoparticles: synthesis characterization and applications. *Journal of microbiological methods*. 2019 163:105656.
- [20] Thakkar Kaushik, Mhatre Snehit, and Parikh Rasesh. Biological synthesis of metallic nanoparticles. *Nanomedicine nanotechnology biology and medicine*. 2009 6: 257-62.
- [21] Namvar F, Azizi S, Ahmad MB, Shameli K, Mohamad R, Mahdavi M, and Tahir PM. Green synthesis and characterization of gold nanoparticles using the marine macroalgae *Sargassum muticum*. *Res Chemical Intermediates*. 2015 41(8):5723-30.
- [22] Ebrahiminezhad Alireza, Bagheri, Mahboobeh, Taghizadeh, Seyedeh-Masoumeh, Berenjian, Aydin, and Ghasem Younes. Biomimetic synthesis of silver nanoparticles using microalgal secretory carbohydrates as a novel anticancer and antimicrobial. *Advances in Natural Sciences Nanoscience and Nanotechnology*. 2016 7(1): 015018.
- [23] Haliza Katas, Noor Zianah Moden, Chei Sin Lim, Terence Celesistinus, Jie Yee Chan, Pavitra Ganasan, and Sundos Suleman Ismail Abdalla. Biosynthesis and Potential Applications of Silver and Gold Nanoparticles and Their Chitosan-Based Nanocomposites in Nanomedicine. *Hindawi Journal of Nanotechnology*. 2018: 1-13.
- [24] Zhi-Qi Wu, Yan-Yan Liu, Fang Ni, Wei-Juan Song, Erfu Xie, Hemant Goyal, Hua-Guo Xu. Evaluation of preliminary screening strategies for human immunodeficiency virus: a single center experience. *Journal of Laboratory and Precision Medicine*. 2017 2: 50.
- [25] Dane Bowder, Haley Hollingsead, Kate Durst, Duoyi Hu, Wenzhong Wei, Joshua Wiggins, Halima Medjahed, Andrés Finzi, Joseph Sodroski, and Shi-Hua Xiang. Contribution of the gp120 V3 loop to envelope glycoprotein trimer stability in primate immunodeficiency viruses. *Virology*. 2018 521: 158–168.
- [26] Tamer Shoeib, K. W. Michael Siu, Alan C. Hopkinson. Silver Ion Binding Energies of Amino Acids: Use of Theory to Assess the Validity of Experimental Silver Ion Basicities Obtained from the Kinetic Method. *The Journal of Physical Chemistry A*. 2002 106: 6121-6128